

## Time-lapse geophysics for monitoring an infiltration test in the vadose zone

A. GODIO<sup>1</sup> and S. FERRARIS<sup>2</sup>

<sup>1</sup> *Facoltà Ingegneria, Ditag, Politecnico di Torino, Italy*

<sup>2</sup> *Facoltà Agraria, Deiafa, Università di Torino, Italy*

(Received September 6, 2004; accepted March 22, 2005)

**ABSTRACT** The flow condition in the vadose zone was monitored by taking measurements of the electromagnetic properties of the subsoil (electrical conductivity and permittivity) to estimate the spatial distribution of the volumetric water content. A controlled experiment of 4x1 m<sup>2</sup> of pond infiltration was designed and done in a sandy soil; the time-lapse electrical resistivity tomography (TLERT) was integrated by Time Domain Reflectometry (TDR) electromagnetic monitoring to analyze variations of water content. The results permitted us to estimate the water-content distribution up to a 2 m depth with accurate lateral detail; because of the duration of the experiments (85 days), several rainfall events modified the water contents of the subsoil: however, the combined approach (TDR and TLERT) permitted us to recognize the different water-content conditions in the zone of artificial infiltration. The interpretation of the experiment has been realised combining the geophysical interpretation and the results of a 2-D simulation of the flow in an unsaturated zone using numerical models.

### 1. Introduction

Non-invasive geophysical measurements are widely used for monitoring time and spatial changes of physical parameters of the subsoil for environmental or hydrogeological purposes. For instance, the analysis of flow conditions is of primary importance to assess the vulnerability of the subsoil subjected to contamination from the surface. Geophysical methods can integrate conventional approaches to assess the flow condition in the vadose zone, because the electromagnetic properties of the subsoil (electrical conductivity and permittivity) can be related to the volumetric water content.

The monitoring of infiltration tests is focused on the analysis of the time and spatial evolution of water in the vadose zone; the final aim is to estimate the distribution of water content in the subsoil and determine vertical flow in the unsaturated zone for the assessment of aquifer vulnerability (Park, 1998). Experiments to map the flow of water from the ground surface downwards through the unsaturated zone and into the water table were described by Barker and Moore (1998). Park (1998) reported the results of a field experiment to detect fluid migration in the vadose zone by 3-D inversion of resistivity monitoring data. The results confirmed that inversion of resistivity data may be useful to monitor fluid migration in the vadose zone; otherwise, independent confirmation of moisture contents were not available and, therefore, any relationship between saturation changes and resistivity changes was not proven.

Simulations of unsaturated flow and solute transport in soil, typically, use closed-form functional relationships to represent water-retention characteristics and unsaturated hydraulic conductivities. The Gardner and Russo exponential model (Russo, 1988), the Brooks and

Corey (1964) model, and the van Genuchten (1980) model represent some of the most widely used and practical hydraulic property models; these parameter models are valid at the Darcian scale. When these models are used in larger scale (plot, field, watershed, or regional) processes, it is necessary to use them in a distributed way. Instead, major questions remain about how to average the spatially variable hydraulic properties over a heterogeneous soil volume (e.g., Russo, 1992; Desbarats, 1998). During the past two decades, many research efforts have been dedicated to this issue, and the problem is usually analysed using stochastic models.

Monitoring of groundwater flow after heavy rainfalls in landslide-slope areas was investigated by means of 2-D inversion of resistivity data in heavily weathered rocks with an extensive shear-zone several tens of meters thick (Suzuki and Higaschi, 2001). The results suggested a good correlation between the resistivity decrease and the infiltration of rainwater. Studies were focused on monitoring salt tracer flow in jointed rocks; they suggested that the groundwater flow could be detected more easily in porous unconsolidated sediments than in virgin, jointed rocks.

In sandy soil, with low content of clay materials, the electromagnetic parameters are influenced by the geometric distribution of water in the subsurface; this causes the relationship between the electromagnetic properties and water content to become scale-dependent in complex geological systems. Moysey and Knight (2004) derived dielectric constant versus water content relationships that account for subsurface geometry in spatially correlated random media that can be characterised using geostatistics. The importance of scale effects are strongly dependent on the variance and the anisotropy of the water content in the subsurface; in some cases, ignoring scale effects will not significantly impact the estimation of water content, while in other cases, large biases can occur. They provide a conceptual framework for the predictive modelling of field-scale dielectric constant vs. water content relationships.

Experiments for monitoring the moisture contents of the vadose zone were conducted by Kean *et al.* (1987) by using DC resistivity soundings; they have proven the reliability of the empirical relationship (Archie law) between changes of moisture contents in sandy soil and electrical resistivity changes. Kean *et al.* (1987) pointed out that the changes of resistivity with soil moisture are also related to the amount of silt and/or clay material. They verified that small changes of soil moisture provided for great variations of resistivity changes in soil with a small amount of clay or silt.

The experimental validation of such approaches remains a developing task of research; the aim of the experiment described in this paper is to verify the reliability of a combined geophysical approach to calibrate the parameters of a distributed Richards equation model for the water saturation modelling of a vadose zone (Manzini and Ferraris, 2004). This issue was addressed by means of an experiment of infiltration in a well characterised by sandy soil. The following redistribution and rainfall infiltration was monitored by integration of time-lapse electrical resistivity tomography and Time Domain Reflectometry (TDR) measurements.

## 2. Materials and methods

The site is characterised by a regular stratigraphic sequence of sandy soil caused by wind transport; the unsaturated zone has a porosity ranging between 0.35 and 0.4, high vertical permeability and low organic content; therefore, the area represents an ideal test site for

percolation studies. The water table is at a deeper level, at about 20 m depth and therefore, no influence of the saturated zone must be taken into account in the experiment interpretation. According to the Comprehensive Soil Classification System, two primary horizons are recognised: up to 1.2 m in depth the A-horizon of mineral matter (80% sand, 14% silt and 6% clay) with average porosity of 0.4 and cationic exchange capacity (CEC) of 4 meq/100 g; from 1.2 up to 2 m in depth the C-horizon of partially altered material (95% sand, 3% silt and 2% clay) with porosity of 0.35 and CEC=0 meq/100 g. Following Clavier *et al.* (1977), the effective porosity, taking into account the increase of tortuosity due to the bound water for the presence of clay material in sandy matrix, is, in this case, approximately 2% less than the total porosity.

The controlled experiment refers to a 4 x 1 m<sup>2</sup> pond infiltration of 2.14 m<sup>3</sup> of water at a temperature of 7°C and electrical conductivity of 200 mS/cm; the infiltration time was of 28 min. approximately, at a constant rate.

The experiment's objective is to verify the effectiveness and the resolution of an integrated geophysical monitoring of water flow in the vadose zone and the reliability of determining changes of saturation by the integration of geophysical data and modelling results. For this reason, an independent monitoring of water content is needed. Therefore, the tools adopted in the study are:

- time-lapse electrical resistivity tomography to monitor resistivity changes with time during the infiltration of a controlled volume of fresh water, using the multielectrode system;
- monitoring of water content by means of TDR measure of electrical permittivity at different depth and at different time during the infiltration;
- modelling of the infiltration by a 2-D numerical solution of Richards equation.

The multielectrode devices for automatic electrical resistivity tomography were developed in the last decade; these devices have permitted us to monitor field experiments of flow and transport in the vadose zone in different test sites (Barker, 1996). Infiltration experiments are well documented and monitored using a combined approach of TDR measurements and resistivity tomography (Hagrey and Michaelsen, 1999).

The experiment discussed here was focused to monitor water infiltration in sand for a visualisation of the water flow up to a 3 m depth.

The electrical resistivity monitoring of the infiltration was carried out by an array of 48 electrodes along a single transect close to the pond (Fig. 1); the infiltration zone was located in the middle of the transect. The distance between the electrodes was 0.6 m for a total length of about 28 m. This arrangement theoretically guarantees an investigation depth in the central part of the vertical section of about 4-5 m. Electrical measurements were realised using a Wenner-Schlumberger with 529 measurements. Measurements were acquired at different times, before and after the infiltration, for about 85 days, in the spring of 2003. We adopted a Syscal Junior Iris Instruments with a maximum power of 100 W and a resolution of 0.5%; the measurement reproducibility was very high and we discharged only few data for each data set, with inaccuracy higher than 0.05.

TDR is an indirect method for measuring soil water content (e.g. Topp *et al.*, 1980). It is based on the measurement of the travel time of an electromagnetic impulse along a transmission line inserted into the soil. The propagation velocity ( $v$ ) of an electromagnetic wave along the transmission line (waveguide) of length  $L$ , embedded in the soil, depends on the electromagnetic



Fig. 1 - Picture of the experimental set-up for infiltration test.

properties of the soil and is a function of the soil bulk dielectric constant ( $\epsilon_b$ ) according to

$$\epsilon_b = \left( \frac{c}{v} \right)^2 = \left( \frac{ct}{2L} \right)^2 \quad (1)$$

where  $c$  is the velocity of electromagnetic waves in vacuum,  $t$  is the travel time for the pulse along the length ( $L$ ) of the embedded rods (forward and backward). The soil bulk dielectric constant ( $\epsilon_b$ ) is governed by the quantity of liquid water (its permittivity is  $\epsilon_w = 81$ , while the ones of other soil constituents are much smaller, e.g., soil minerals  $\epsilon_s = 3$  to 5 and air  $\epsilon_a = 1$ ). This large disparity of the dielectric constants makes the method relatively insensitive to soil composition and texture and thus a good method for liquid soil water measurement. The dielectric constant is only slightly affected by temperature and salt concentration of the subsoil and, therefore, the water content estimate is more accurate than methods based on resistivity evaluation only.

One-meter and two-meter long couples of vertically inserted TDR rods were located at 1 m horizontal intervals along the same transect of the time-lapse electrical resistivity tomographic (TLERT) measurements, starting from coordinate 12.5 m up to 16.5 m of the electrical transect, namely just outside the longer boundary of the pond. Other 8 couples of vertical TDR probes ranging between a 0.15 m and 2 m length were infixed inside the pond after the disappearance of free surface water. The Tektronix 1502b instrument was adopted; the equipment is characterised by a time resolution of 0.1 ns, that means a theoretical accuracy on electric permittivity estimation less than 5%.

An accurate model of the subsurface can be obtained: it is a two-dimensional (2-D) section where the resistivity changes in the vertical direction as well as in the horizontal direction along the survey line, using the electrical tomographic approach. In theory, a 3-D resistivity survey and

interpretation model should be even more accurate. However, at the present time, for the analysis of the infiltration process, the 2-D survey represents a practical and economic compromise between result accuracy and acquisition times. In sandy soil with reduced clay fraction, where vertical hydraulic conductivity is very high, the influence of changes of soil moisture during the acquisition of a single section may significantly affect the reliability of the monitoring. Therefore, we acquired each single section in less than 20 minutes.

The result of the electrical tomography is an image of 2-D distribution of electrical resistivity in a vertical plane. A preliminary overview of the infiltration process can be performed by imaging of the ratio between the observed data at different times during the experiment; this approach reduces the ambiguities in the evaluation of the resistivity changes caused by the infiltration process. However, the final interpretation of water content is based on the results of real resistivity values as computed by tomographic inversion.

The electrical resistivity of subsoil depends on porosity, water content (saturation), water salinity and contribution of clay particles. Archie type equations usually produce accurate water saturation values when  $m$  (cementation factor), and  $n$  (saturation exponent) can be measured or known. These factors vary with rock type, porosity and conductivity path. For shaly sands, accurate water saturation values are best obtained when effective clay conductivity is accounted for; therefore, Waxman and Smits equations are used to account for clay conductance, because they take into account the CEC of the soil and the soil salinity.

To interpret the resistivity data, we adopted the correlation between porosity, saturation and electrical conductivity at low frequency based on the Waxman-Smits model (Waxman and Thomas, 1974).

Park and Dickey (1989) discussed the physical model of electrical conduction in the vadose zone in detail: electrolytic conduction and surface conduction of clay particles are the main mechanisms for electrical conduction at a low frequency. Electrolytic conduction permits the current conduction through the electrolytic solution, filling the pore volumes of sediments. It affects the in-phase response. Clay conduction produces a response both in-phase and out of phase with the current source (Ward, 1967). Vinegar and Waxman (1984) proposed that the complex conductivity of a clay-rich saturated sediment could be approximated by the following relationship:

$$\sigma_{rock}^* = \sigma_w \cdot \phi^m + \sigma_{clay}^* \quad (2)$$

where the asterisk denotes a mathematically complex quantity. The relationships between the in-phase and quadrature conductivity and the petrophysical parameters were also derived:

$$\sigma_{phase} = \frac{\sigma_w + BQ_v}{F} \quad (3)$$

$$\sigma_{quad} = \frac{\lambda Q_v}{F\phi} \quad (4)$$

where  $F$  is the formation resistivity factor;  $B$  is the equivalent conductance of the cations;  $\lambda$  is the equivalent quadrature conductance and  $Q_v$  is the cation exchange capacity per unit pore volume. The equivalent conductance is dependent principally upon the solution conductivity  $\sigma_w$ ;

therefore, it depends on the water temperature ( $T_{\text{water}} = 7^\circ\text{C}$  and  $\sigma_w = 0.02 \pm 0.001 \text{ S/m}$ ). We assume that water temperature changes are not relevant at least in the first few days of the start of the infiltration test:

$$B = 3.83 \cdot [1 - 0.83\exp(-0.5 \cdot \sigma_w)] \quad (5) \quad (S \times \text{cm}^2/\text{geq})$$

and the shalyness parameter  $Q_v$  takes into account the effect of cation exchange capacity (CEC in meq/100 g of soil) due to the clay fraction:

$$Q_v = \frac{1-\phi}{\phi} \frac{d_s}{100} \text{CEC} \quad (6) \quad (\text{meq}/\text{cm}^3)$$

where  $d_s$  is the bulk density ( $\text{g}/\text{cm}^3$ ) and  $\phi$  is the soil porosity.

In the vadose zone, for an unsaturated medium, the in-phase response can be modified according to the saturation term:

$$\sigma_{\text{phase}} = \frac{S_w^n}{F} \left( \sigma_w + \frac{BQ_v}{S_w} \right) \quad (7)$$

where  $n$  is the saturation exponent usually in the range between 1.2 and 2.5.

We assume that the conductivity of the electrolytic solution does not change during the infiltration process; the spatial variations of the formation factor  $F$  and of parameters  $B$  and  $Q_v$  are negligible. Therefore, the ratio of conductivity at different times reduces the previous equation to a ratio of saturation values:

$$\frac{\sigma_1}{\sigma_0} \Leftrightarrow \frac{F \cdot S_{w,1}^n}{F \cdot S_{w,0}^n} \Leftrightarrow \frac{S_{w,1}^n}{S_{w,0}^n} \quad (8)$$

The model is very sensitive to the value of  $n$ -exponent for low saturation (less than 0.4) and high bulk resistivity; otherwise for high saturation degree and low bulk resistivity the model sensitivity to  $n$ -exponent is strongly reduced. This task is pointed out by the plot of Fig. 2, where the bulk (soil) resistivity for different values of  $n$ -exponent and for a soil with matrix density of  $2.7 \text{ (g}/\text{cm}^3)$ , with a cation exchange capacity  $\text{CEC} = 4 \text{ (meq}/100 \text{ g)}$ , a porosity  $\phi = 0.4$  and fluid resistivity of  $50 \text{ (ohm} \cdot \text{m)}$  is plotted versus the saturation. Therefore, the estimation of the  $n$ -exponent could be a critical point in the final interpretation of the soil moisture changes.

To estimate the sensitivity of the model to changes of CEC, we can analyze the plot of Fig. 3 where the trend of bulk resistivity versus water saturation is plotted for a medium of porosity 0.3, a water resistivity of  $50 \text{ ohm} \cdot \text{m}$ , similar to the actual condition of the subsoil of the experiment. A great variability of bulk resistivity values can be assessed for a decrease of CEC values; for instance for a saturation of 0.4, resistivity values increase from  $130 \text{ ohm} \cdot \text{m}$  up to  $500 \text{ ohm} \cdot \text{m}$  for a decrease of CEC in the range between 5 and 1 meq/100 g.

To analyse the reliability of 2-D resistivity tomography to monitor the effect on the fluid migration, we model the theoretical response of 2-D resistivity tomography for a Wenner-Schlumberger array. For dry conditions, the reference model is characterised by a two-layer subsoil with a near-surface more resistive layer ( $1000 \text{ ohm} \cdot \text{m}$ ) and a deeper less resistive layer

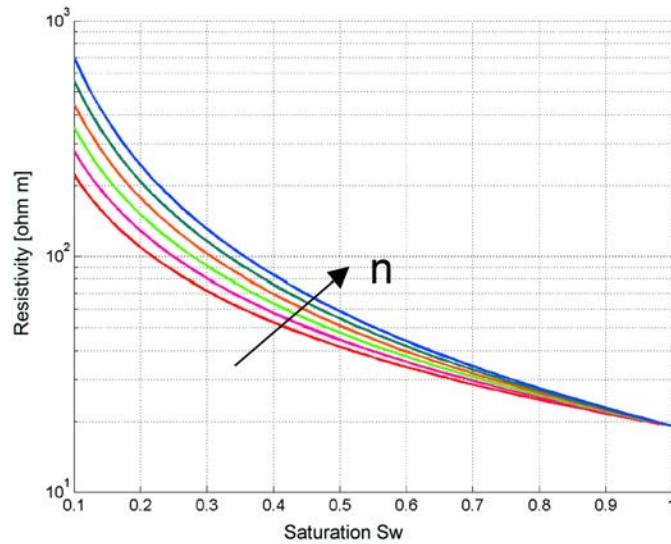


Fig. 2 - Resistivity vs. water saturation for a porosity 0.3, CEC value of 4 meq/100 g and for a water resistivity of 50 ohm·m (cementation factor  $m = 2$ ) to increase values of  $n$ -exponent in the range 1.2-2.2 with increment of 0.2.

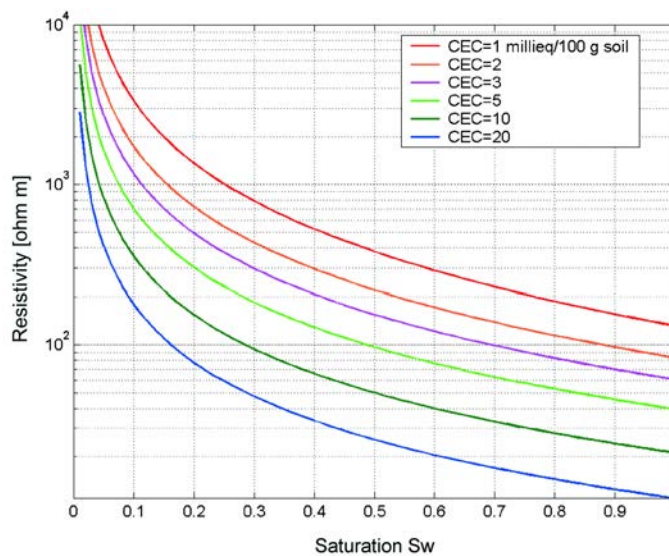


Fig. 3 - Resistivity vs. water saturation for different values of CEC; water resistivity of 50 ohm·m (cementation factor  $m = 2$ ), porosity = 0.3.

(200 ohm·m). The effect of changes of subsoil saturation is modelled with different blocks of a conductive target, where true resistivity of the target is calculated according to the hypothesis of saturation changes in the range between 0.2 up to 1 and for reference values of  $n$ -exponent equal to 2.2 (porosity=0,3; cementation factor  $m = 2$ , CEC=4 meq/100 g and water resistivity 50 ohm·m).

We discuss the results of the different modelling steps computed to simulate an infiltration with a saturation above 0.8 and correspondent resistivity values of 50 ohm·m. Three different

steps are plotted in Fig. 4, with the front of infiltration at a depth of 0.2 m, 1.0 m and 2.0 m. The model considers a uniform saturation on the infiltrated area. It can be noticed that a good horizontal resolution during the infiltration test can be obtained using the Wenner-Schlumberger array. We have considered that the dipole-dipole array should offer a better resolution than the Wenner-Schlumberger one; unfortunately, the preliminary tests on site have verified a high noise level in the data set related to the dry condition of the near-surface layer. Therefore, the dipole-dipole array has not been adopted in this experiment.

As concerns the empirical relationship between water content  $\theta$  and dielectric constant, the Topp *et al.* (1980) relationship is adopted in this study:

$$\theta = -5.3 \cdot 10^{-2} + 2.92 \cdot 10^{-2} \varepsilon_b + 5.5 \cdot 10^{-4} \varepsilon_b^2 + 4.3 \cdot 10^{-6} \varepsilon_b^3 \tag{9}$$

The relationship for mineral soils provides an adequate description for the water content range  $<0.5$  (which is the entire range of interest in most mineral soils). Following the literature, the accuracy of the Topp *et al.* (1980) formula in an application like ours can be about 2-3%.

The water flow out of the pond in a variably saturated, isotropic, rigid soil can be modelled by the following form of Richards' equation:

$$\frac{\partial \theta}{\partial t} = \frac{\partial}{\partial x} \left( K \frac{\partial h}{\partial x} \right) + \frac{\partial}{\partial z} \left( K \frac{\partial h}{\partial z} \right) - \frac{\partial K}{\partial z} \tag{10}$$

where  $\theta (L^3L^{-3})$  is the volumetric water content ( $\phi S_w$ ),  $h (L)$  is the pressure head,  $K (LT^{-1})$  is the hydraulic conductivity,  $x (L)$  is the horizontal coordinate along the transect direction,  $z (L)$  is the vertical coordinate positive downward. Eq. (10) is solved numerically for the following initial and boundary conditions:

$$h(r, z, 0) = h_i \tag{11a}$$

$$h(r, 0, t) = h_0 \quad 12.5 \text{ m} \leq x \leq 16.5 \text{ m} \quad t < t_f \tag{11b}$$

$$\text{atmospheric b.c.} \quad z = 0 \quad x < 12.5 \text{ m}, x > 16.5 \text{ m} \quad t < t_f, \forall x \text{ if } t < t_f \tag{11c}$$

$$\frac{\partial h}{\partial z} = 1 \quad z = z_b \tag{11d}$$

$$\frac{\partial h}{\partial x} = 0 \quad x = x_b \tag{11e}$$

where  $h_i (L)$  is the initial pressure head and  $x_b$  and  $z_b$  are the coordinates of the flow domain boundaries. The soil surface is modelled by atmospheric boundary conditions with the exception of the pond, while free surface water is present. The atmospheric b.c.'s are the combination of fixed pressure head and fixed gradient conditions, switching between them in relation to the soil-surface, time-variable, pressure-head values.

A finite volume code was used (Manzini and Ferraris, 2004), where time integration is performed by an implicit finite-difference scheme, with automatically variable time steps. The time step at the beginning of the simulation is set by the user and then it is dynamically adjusted



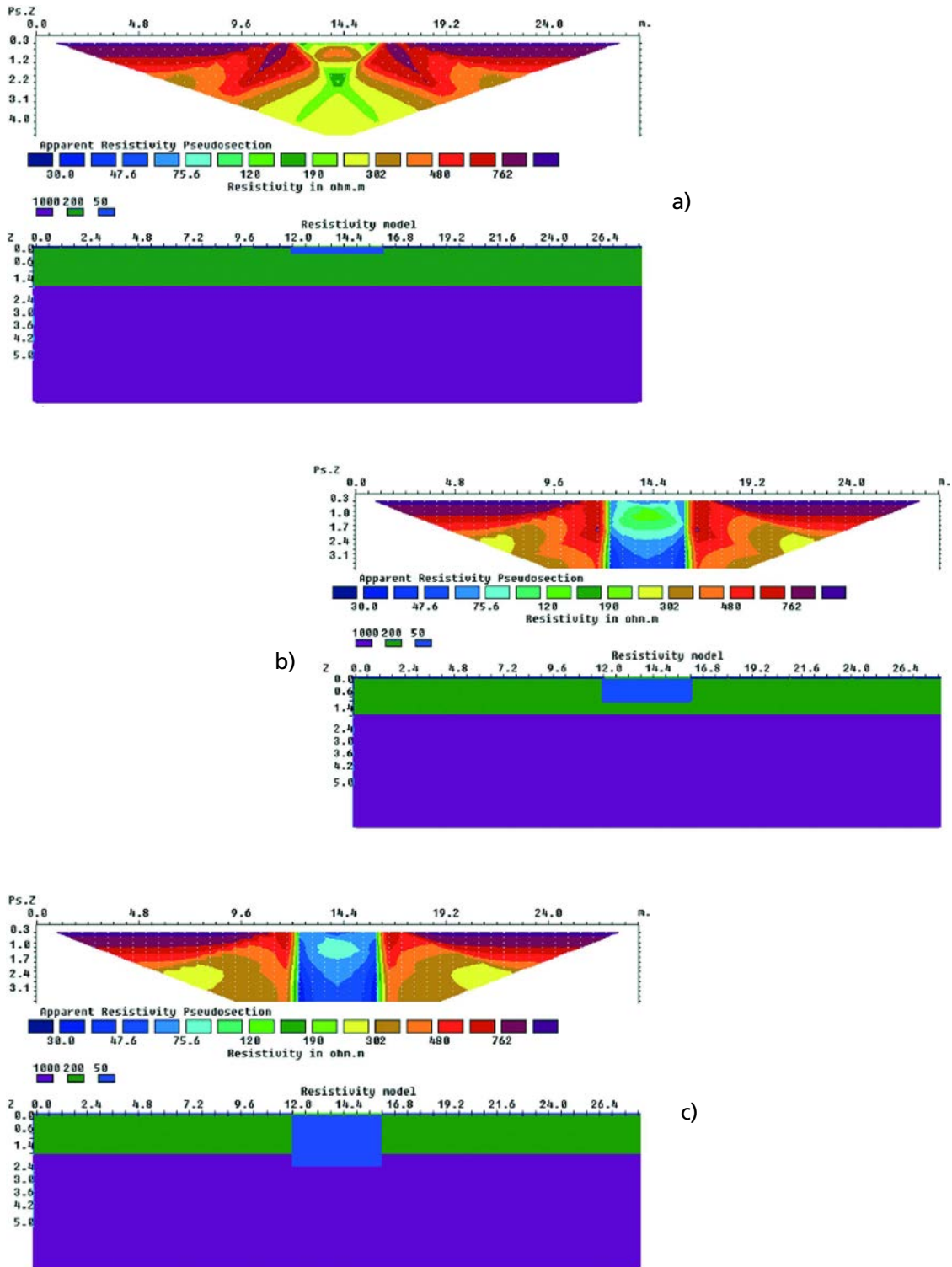


Fig. 4 - Synthetic models of resistivity tomography using a Wenner-Schlumberger array: a) simulation of an infiltration of a conductive flow up to a depth of 0.2 m; b) infiltration at 1.0 m depth; c) infiltration at 2.0 m.

using increasing and decreasing factors, according to the convergence behavior. As convergence problems usually occur at the beginning of the infiltration, the initial time step was set equal to the minimum time step,  $t_{min}$ . A structured grid was generated in order to discretise the vertical transect in space.

The van Genuchten-Mualem model (VGM model) was used to describe the soil hydraulic properties (van Genuchten, 1980):

$$S_e(h) = \frac{\theta - \theta_r}{\theta_s - \theta_r} = \left[ 1 + \left( \frac{h}{h_g} \right)^n \right]^{-m} \quad (12)$$

$$K(\theta) = K_s S_e \left[ 1 - (1 - S_e^{1/m})^m \right]^2 \quad (13)$$

where  $S_e$  (-) is the effective saturation,  $\theta_s$  ( $L^3L^{-3}$ ) is the saturated water content,  $\theta_r$  ( $L^3L^{-3}$ ) is the residual water content,  $h_g$  (L),  $n$  (-) and  $m$  (-) are empirical parameters with  $m = 1 - 1/n$  (Mualem, 1976).

Simulations were also conducted by the van Genuchten (1980) equation for water retention with the Burdine (1953) expression for the  $m$  parameter ( $m = 1 - 2/n$ ), coupled with the Brooks and Corey (1964) equation for hydraulic conductivity (VGB model):

$$K = K_s S_e^c \quad (12)$$

where  $c$  is a fitting parameter.

### 3. Results and discussion

The initial electrical pseudosection before the infiltration is characterized by a regular distribution of the apparent resistivity; the upper resistive layer shows values higher than 1000 ohm·m. due to the presence of high porosity and very dry conditions. For higher electrode spacing (and therefore higher pseudosection depth) the apparent resistivity decreases to 500-600 ohm·m. Twenty minutes after the infiltration start the difference between the step and the pre-infiltration pseudosections pointed out a conductive anomaly of about 500 ohm·m. The two lateral resistive anomalies close to the conductive target are, instead, the artefact effect typical of the adopted electrode array. The sequence of pseudosections (30 – 60 – 120 ... 480 min after the infiltration) reflects the downward flow of the water front with time, showing a higher conductive anomaly in the upper horizon well closed to the middle of the resistivity image (Fig. 5). The two lateral high resistive anomalies are enhanced in these pseudosections; their shape is very similar to that estimated using a Wenner-Slumberger array, as can be obtained by the forward modelling solution on synthetic examples, previously discussed.

One day after the infiltration the high conductive zone on the upper horizon begins to decrease slowly; a slight conductive effect could be depicted after a few days, up to 70 days from the infiltration; 85 days after the infiltration, any conductive anomaly is no longer evident, according

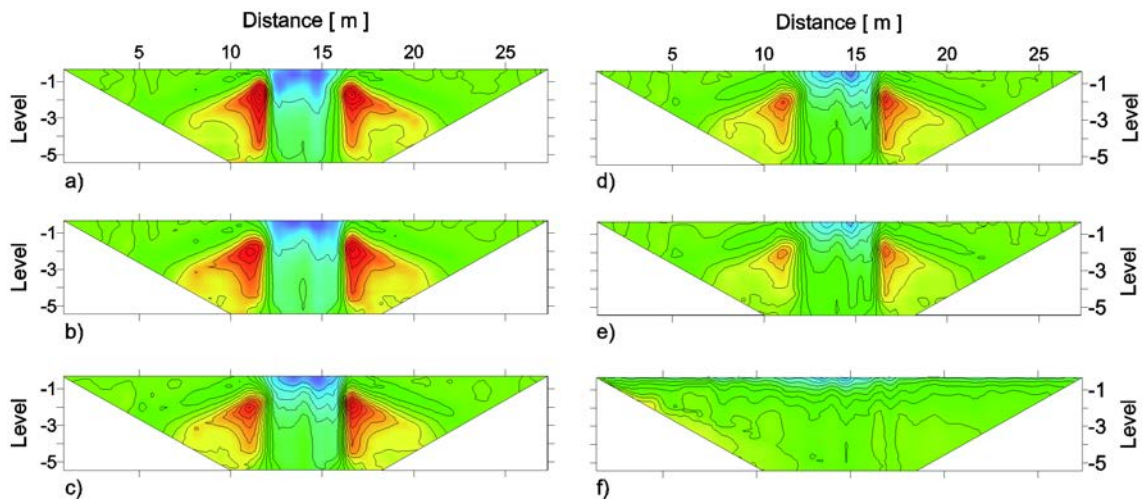


Fig. 5 - Pseudosections of differences of resistivity values at different monitoring time with respect to the pre-infiltration condition: a) 30 minutes after the infiltration; b) 120 minutes; c) 420 minutes; d) 1400 minutes; e) 4 days; f) 70 days.

to the dry conditions of the upper horizon due to the evapo-transpiration process at the surface, for warm climate conditions.

During the monitoring period, few rainfall events occurred for a total amount of 45 mm of rain; the effect of rainfall is particularly evident in the acquired data after 28 days from the infiltration. The upper horizon shows a homogeneous decrease of resistivity caused by the infiltration of water due to the rainfall, according to previous studies (Benderitter and Schott, 1999).

The results of inversion are presented in Fig. 6; the inversion has been carried out by using the ProfileR code. The software (Binley, 2003) has been designed for surface array resistivity profile imaging, permitting an inverse solution for a 2-D resistivity distribution based on the computation of a 3-D current flow using a quadrilateral finite element mesh. The inverse solution is based on a regularised objective function combined with weighted least-squares.

A solution using an Occam type inversion is preferred in order to take into account the gradual changes of resistivity according to the smoothing variation of saturation in the subsoil. Changes in moisture content, porosity, cation exchange capacity, solutes in the pore water, and temperature, influence the resistivity of the soil. In the following analysis, we assume that only the moisture content is important because these are the only two parameters that are likely to change during the infiltration test. If the only change caused by the infiltration is a saturation increase, then the bulk electrical resistivity will typically decrease. through the analysis of time-lapse resistivity data, the effect of CEC becomes negligible and the temperature effect can be minimized if only the first few days of the experiment are considered.

The analysis of the inverted section, as reported in Fig. 7, pointed out the sensitivity of the method to the vertical flow in the vadose zone.

From a qualitative point of view, within the approximated limits of applying 2-D data processing for flow structures assumed to be 3-D, the resistivity tomographic inversion has

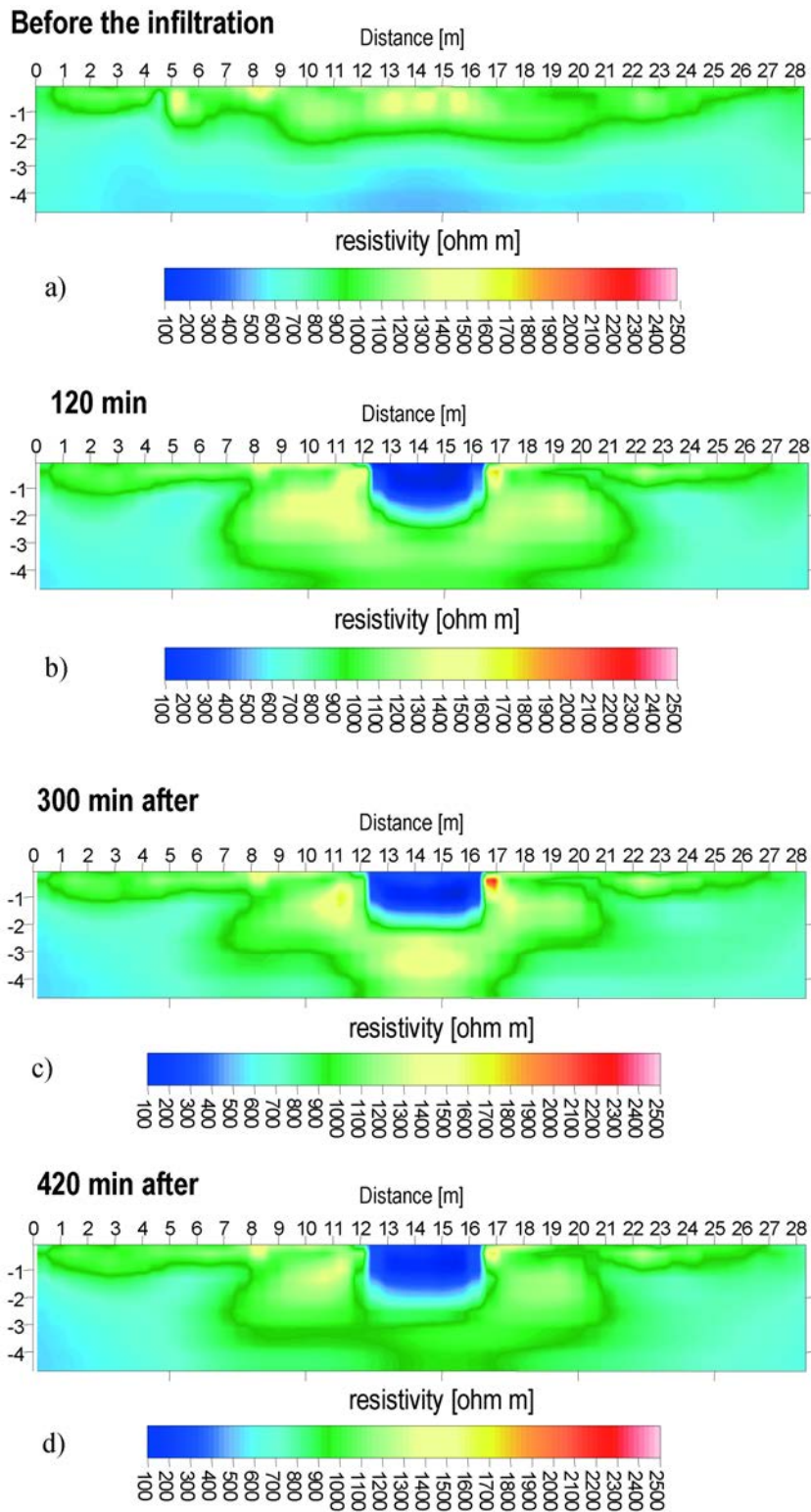


Fig. 6 - Resistivity models for different steps of the experiment derived from Occam's inversion: a) before the infiltration; b) after 120 min; c) after 300 min; d) after 420 min.

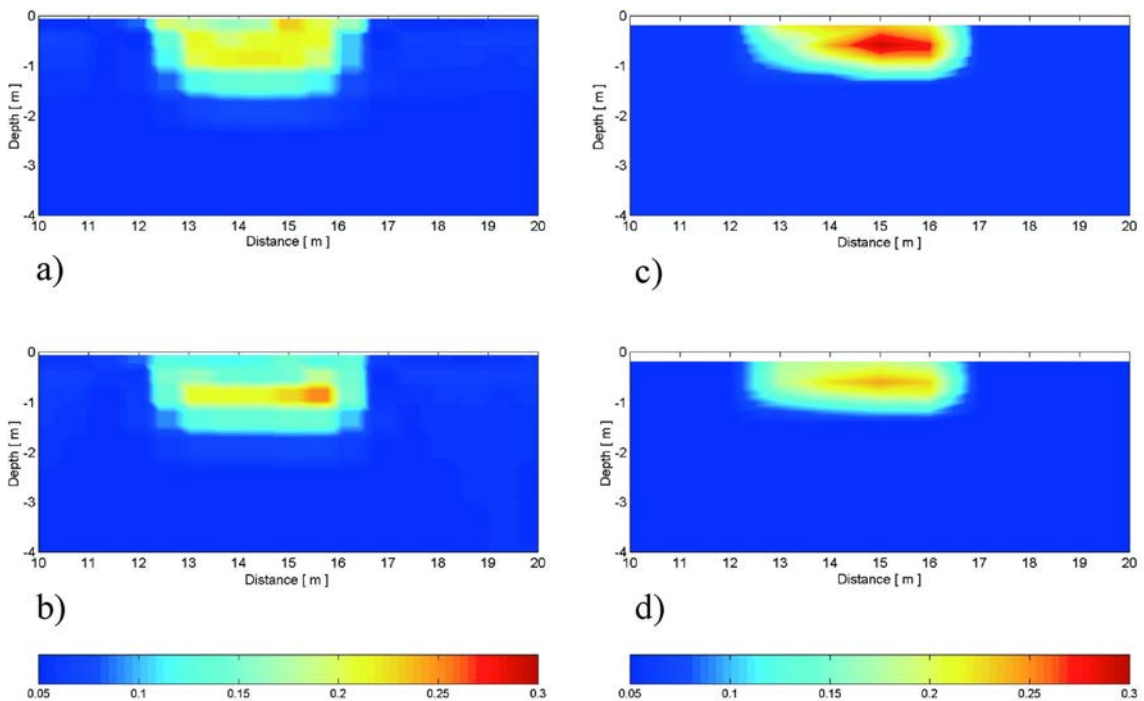


Fig. 7 - Comparison between water-content distribution after 120 and 300 min estimated by the analysis of electrical resistivity tomography (a) and (c) and by solution of Richards equation (b) and (d).

detected and imaged the infiltration in the sub-surface. It can be considered that for a depth greater than 2 meters the flow encountered a layer with a background of water content characterised by high values (but not saturated) that do not permit us to determine significant changes in saturation starting from the resistivity image. Two effects can be considered: the hydraulic conductivity decreases according to the high values of saturation; the resolution of the electrical resistivity tomography decreases with depth. Therefore, the effect of low vertical flow velocity and lack of resolution of the electrical resistivity tomography do not permit quantitative information by time-lapse analysis at a deeper layer to be determined.

The quantitative analysis of the inverted sections permits the following consideration:

- before the infiltration, two main layers with sharp resistivity variation at a depth of 1-2 m can be recognised; the near-surface horizon is characterised by resistivity in the range of 1100 and 1400  $\text{ohm} \cdot \text{m}$ ; this result is consistent with saturation values less than 0.1 (for CEC of 4  $\text{meq}/100 \text{ g}$ ) and water content less than 0.04. From TDR measurements, average values of  $0.06 \pm 0.01$  have been estimated;
- after the infiltration, at 120 min, the bulk resistivity of the zone touched by the infiltration is about 100  $\text{ohm} \cdot \text{m}$ ; after 300 min the resistivity images at the front of the infiltration reached a depth of 1.5-2 m and after 420 min the low resistivity zone reached the depth of about 2 m. The resistivity values of the conductive bulb are not lower than 100  $\text{ohm} \cdot \text{m}$ ; according to the theoretical evaluation based on the Waxman-Smits model the total saturation is not reached. TDR measurements pointed out a water content of 0.21-0.23 at 1 m in depth and 0.2 at 2 m in

depth after 300 min; a decrease of water content is observed after 420 min at the depth of 1 m (water content of 0.15-0.16); the value of 0.2-0.22 is observed at 2 m in depth.

To estimate the water content during the experiment by resistivity data Eq. (8) was used, starting from an initial (before infiltration) average value of 0.06. Furthermore, the reliability of water content estimation from resistivity data was validated using TDR measurements. The sequence of the inverted models offers a good imaging of the different depths reached by the water front at different times during the infiltration, permitting us to verify the absence of preferential vertical pathways in the subsoil interested by the infiltration. According to this experimental evidence, we propose a 2-D modelling of the flow using a numerical solution of the Richards equation. The dominion of the numerical solution has been extended up to 4 m in depth, along a vertical section, corresponding to the TLERT vertical section.

The hydraulic modelling of the flow was performed considering the saturated water content  $\theta_s = 0.045$ , the residual water content,  $\theta_r = 0.38$ , the van Genuchten parameter  $\alpha = 14.5 \text{ (m}^{-1}\text{)}$  and  $n = 2$ . The hydraulic conductivity in saturated condition is  $K_s = 0.003 \text{ (m/h)}$ .

The model has been calibrated according to the results of the TDR monitoring using the comparison between the 2-D section of soil-water content values estimated by the model and the water content derived by TLERT.

The comparison between the water content estimated by resistivity data and the water content distribution determined by 2-D flow modelling is reported in Fig. 7. For brevity, the simulation results refer to the situation after 120 min and 300 min from the infiltration.

A slight difference between the hydraulic simulation and the water content estimated by time-lapse resistivity data can be observed; this is partially related to the inaccuracy in the estimation of the  $n$ -factor in Eq. (8).

The model, that refers to the situation after 24 hours from the application of water from the surface, indicated that the vertical flow reached a depth above 2 m, according to high vertical hydraulic conductivity of the sandy soil. After this period the divergence between the experimental and simulated data due to local changes of porosity and hydraulic conductivity of deeper level does not permit us to control the test.

#### 4. Final remarks

The controlled experiment of water infiltration was monitored by an integrated geophysical approach using electrical tomography, TDR data and hydraulic simulation, in order to estimate the water-flow in a sandy soil. This joint approach is not completely new in the monitoring of water flow in vadose zone (Dannowski and Yaramanci, 1999); however, the combination of geophysical monitoring and numerical model of flow is very promising for a detailed description of the phenomena in the vadose zone.

The results permitted us to estimate the water content distribution up to 2 m in depth with accurate lateral detail. The test verified the reliability of geophysical data to estimate the 2-D water-content distribution in the subsoil; the possibility of this approach to calibrate the modelling of vertical flow in the vadose zone using a numerical model is also proposed.

A critical point of the suggested approach is the difficulty of controlling the effect of temperature and salinity changes of the water during the experiment, with negative consequence

on the reliability of the water content, computed from resistivity data. The shortcoming of the accuracy in the evaluation of the saturation exponent of resistivity versus saturation models, remains another ambiguous point; we tried to limit this effect by introducing local constraints derived by estimation of water content through TDR data. The efficiency of the approach could be enhanced by introducing a more accurate evaluation of the saturation exponent of the resistivity-saturation model (e.g Waxman-Smits) improving the statistical reliability of the relationship between TDR and electrical resistivity results.

Alternatively, the combined approach permits an experimental evidence, supplied by modelling calibration, of the water percolation in sandy soil for practical purposes such as vulnerability of the aquifer estimate and for solute transport in vadose zone.

## REFERENCES

- Barker R.D.; 1996: *The application of electrical tomography in groundwater contamination studies*. In: EAGE 58th Conference and Technical Exhibition Extended Abstracts, **1**, P082.
- Barker R. and Moore J.; 1998: *The application of time-lapse electrical tomography in groundwater studies*. The Leading Edge, **17**, 1454-1458.
- Benderitter Y. and Schott J.J.; 1999: *Short variation of the resistivity in an unsaturated soil: the relationship with rainfall*. European Journal of Environmental and Engineering Geophysics, **4**, 37-49.
- Binley A.; 2003: *ProfileR version 2.5 - 2-D inversion of surface resistivity data*. Lancaster University, [www.es.lancs.ac.uk/es/people/teach/amb/Profiler/ProfileR.pdf](http://www.es.lancs.ac.uk/es/people/teach/amb/Profiler/ProfileR.pdf), 8 pp.
- Brooks R.H. and Corey A.T.; 1964: *Hydraulics properties of porous media*. Hydrology paper n.3. Colorado State Univ., Fort Collins, CO, USA, 27 pp.
- Burdine N.T.; 1953: *Relative permeability calculation from pore size distribution data*. Petr. Trans. Am. Inst. Mining Metall. Eng. **198**, 71-77.
- Clavier C., Coates G. and Dumanoir J.; 1977: *The theoretical and experimental basis for the "dual water" model for the interpretation of shaly sands*. Soc. Pet. Eng. Pap., **6859**, 16 pp.
- Dannowski G. and Yaramanci U.; 1999: *Estimation of water content and porosity using combined radar and geoelectrical measurements*. European Journal of Environmental and Engineering Geophysics, **4**, 71-86.
- Desbarats A.J.; 1998: *Scaling of constitutive relationships in unsaturated heterogeneous media: A numerical investigation*. Water Resour. Res., **34**, 1427-1436.
- Hagrey S.A. and Michaelsen J.; 1999: *Resistivity and percolation study of preferential flow in vadose zone at Bokhorst, German*. Geophysics **64**, 746-753.
- Kean W.F., Waller M.J. and Layson H.R.; 1987: *Monitoring moisture migration in the vadose zone with resistivity*. Ground Water, **25**, 562-571.
- Manzini G. and Ferraris S.; 2004: *Mass-conservative finite volume methods on 2-D unstructured grids for the Richards equation*. Advances in Water Resources, **27**, 1199-1215
- Moysey S. and Knight R.; 2004: *Modeling the field-scale relationship between dielectric constant and water content in heterogeneous systems*. Water Resources Research, **40**, W03510, 10 pp.
- Mualem Y.; 1976: *A new model for predicting the hydraulic conductivity of unsaturated porous media*. Water Resour. Res., **12**, 513-522.
- Park S.K. and Dickey S.K.; 1989: *Accurate estimation of conductivity of water from geoelectrical measurements – a new way to correct for clay*. Ground Water, **27**, 786-792.
- Park S.; 1998: *Fluid migration in the vadose zone from 3-D inversion of resistivity monitoring data*. Geophysics, **63**, 41-51.
- Russo D.; 1988: *Determining soil hydraulic properties by parameter estimation: on the selection of a model for the hydraulic properties*. Water Resour. Res., **24**, 453-459.

- Russo D.; 1992: *Upscaling of hydraulic conductivity in partially saturated heterogeneous porous formation*. Water Resour. Res., **28**, 397-409.
- Suzuki K. and Higashi S.; 2001: *Groundwater flow after heavy rain in landslide-slope area from 2-D inversion of resistivity monitoring data*. Geophysics, **66**, 733-743.
- Topp G.C., Davis J.L. and Annan A.P.; 1980: *Electromagnetic determination of soil water content: measurements in coaxial transmission lines*. J. of Water Resources Research **16**, 574-582.
- Vinegar H.J. and Waxman M.H.; 1984: *Induced-polarization of shaly sands*. Geophysics, **49**, 1267-1287.
- van Genuchten M.Th.; 1980: *A closed form equation for predicting the hydraulic conductivity of unsaturated soil*. Soil Sci. Soc. Am. J., **44**, 892-898.
- Ward S.H.; 1967: *Electromagnetic theory for geophysical applications*. In: SEG Mining Comm., Mining Geophysics, 02, Soc. of Expl. Geophys., 10-196.
- Waxman M.H. and Thomas E.C.; 1974: *Electrical conductivities in shaly sands: I. The relation between hydrocarbon saturation and resistivity index; II. The temperature coefficient of electrical conductivity*. J. Petr. Tech., Trans. AIME, **257**, 213-225.

Corresponding author: Alberto Godio  
Politecnico di Torino  
C.so Duca degli Abruzzi 24, 10129 Torino, Italy  
phone: + 39 0115647656; fax: + 39 0115647699; e-mail: alberto.godio@polito.it